





OPEN

High throughput screening of airway constriction in mouse lung slices

Magali Boucher¹, Cyndi Henry¹, Louis G elinas¹, Rosalie Packwood¹, Andr es Rojas-Ruiz¹, Liah Fereydoonzad², Percival Graham² & Ynuk Boss e¹  

The level of airway constriction in thin slices of lung tissue is highly variable. Owing to the labor-intensive nature of these experiments, determining the number of airways to be analyzed in order to allocate a reliable value of constriction in one mouse is challenging. Herein, a new automated device for physiology and image analysis was used to facilitate high throughput screening of airway constriction in lung slices. Airway constriction was first quantified in slices of lungs from male BALB/c mice with and without experimental asthma that were inflated with agarose through the trachea or trans-parenchymal injections. Random sampling simulations were then conducted to determine the number of airways required per mouse to quantify maximal constriction. The constriction of 45 ± 12 airways per mouse in 32 mice were analyzed. Mean maximal constriction was $37.4 \pm 32.0\%$. The agarose inflating technique did not affect the methacholine response. However, the methacholine constriction was affected by experimental asthma ($p = 0.003$), shifting the methacholine concentration–response curve to the right, indicating a decreased sensitivity. Simulations then predicted that approximately 35, 16 and 29 airways per mouse are needed to quantify the maximal constriction mean, standard deviation and coefficient of variation, respectively; these numbers varying between mice and with experimental asthma.

Keywords Airway smooth muscle, Asthma, Contraction, Mouse models, Precision-cut lung slices (PCLS)


Lung slices have been used for decades to study airway constriction¹. Yet, the quantification of airway constriction in lung slices remains time-consuming and labor-intensive. This is not only due to technical challenges of mounting a tiny and frail piece of fresh lung tissue under living conditions where luminal airway narrowing can be visualized during the stimulation of smooth muscle, but also because of the inherently large variability in the level of constriction between airways. This variability is cumbersome as it implies that large sample sizes are required to achieve adequate statistical power.

In the present study, a new automated device for physiology and image analysis, called the physioLens, was used to facilitate high throughput screening of airway constriction in lung slices from male BALB/c mice. Airway constriction was measured and compared between mice with and without experimental asthma. Experimental asthma was induced by repeated exposures to intranasal house-dust mite (an allergen). For both groups, two filling techniques were used to inflate the lung with agarose. The first inflating technique, hereinafter called the traditional technique, consists of infusing agarose into the trachea. The second technique, hereinafter called the needle technique, consists of injecting several boluses of agarose directly through the parenchyma with a needle. Random sampling simulations were then conducted to determine the number of airways to be analyzed in order to allocate reliable values of maximal constriction in one mouse in terms of mean, standard deviation (SD), coefficient of variation (CoV) and median, as well as to determine the extent by which these numbers vary from mouse to mouse and between experimental groups.

Results

Data

Baseline airway dimensions were not different between subgroups of mice (experimental asthma, $p = 0.68$; inflating technique, $p = 0.30$; and interaction, $p = 0.68$). More precisely, when lungs were inflated with the traditional technique, airway diameter was on average 252 ± 57 and 265 ± 53 μm in saline- and HDM-exposed mice,

¹Institut Universitaire de Cardiologie et de Pneumologie de Qu ebec (IUCPO)—Universit e Laval, Pavillon M, room 2687, 2725, chemin Sainte-Foy, Qu ebec, Qc G1V 4G5, Canada. ²SCIREQ Inc., Montreal, QC, Canada. email: ynuk.bosse@criucpq.ulaval.ca

respectively. When lungs were inflated with the needle technique, airway diameter was on average 242 ± 29 and $242 \pm 26 \mu\text{m}$ in saline- and HDM-exposed mice, respectively.

An example of an airway constricting in response to incremental concentration of methacholine is depicted in Fig. 1. A total of 1457 airways were analyzed from 534 lung slices, averaging 2.7 airways per slice. The number of airways analyzed per mouse in each subgroup is shown in Table 1.

The concentration–response curves are depicted in Fig. 2. Neither experimental asthma nor the inflating technique significantly affected the concentration–response curve. However, there was a significant interaction between methacholine and experimental asthma ($p=0.003$), suggesting that experimental asthma altered the methacholine response. On visual inspection, the curves in subgroups with experimental asthma were shifted to the right, and also upwards at the highest concentrations of methacholine. Post-hoc analyses to compare between subgroups at each methacholine concentration indicated that none of these pairwise comparisons were significant.

The mean maximal constriction in all airways was $37.4 \pm 32.0\%$. This level of variability is similar to that reported by others^{2–6}. The mean, SD, CoV and median for each mouse and each subgroup are depicted in Table 1. The results for the mean in each mouse and the average \pm SD of the mean in each subgroup are also depicted in Fig. 3. Neither experimental asthma nor the inflating technique significantly influenced the maximal constriction.

The concentration of methacholine causing 50% of the maximal response (EC₅₀) is depicted in Fig. 4. While the inflating technique did not influence the EC₅₀, experimental asthma significantly increased the EC₅₀, indicating a decreased sensitivity to methacholine.

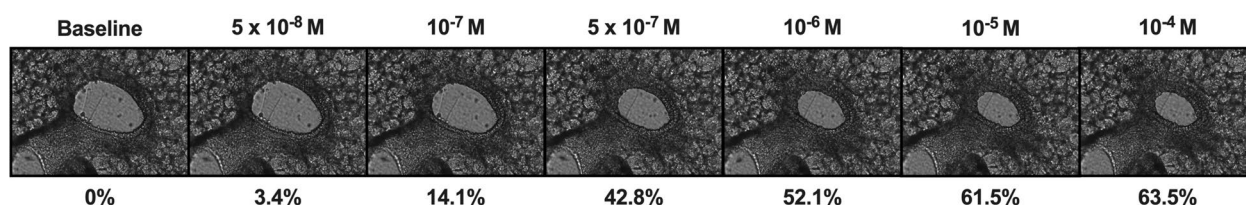
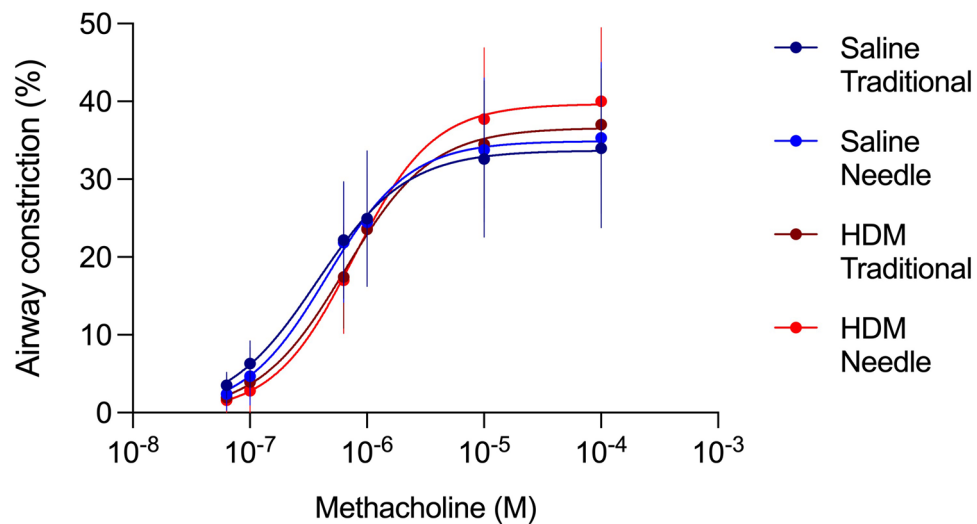


Fig. 1. An example of an airway constricting in response to incremental concentrations of methacholine. Each picture represents the peak constriction captured by the physioLens at each concentration. The methacholine concentration is indicated above each picture. The percentage of constriction is also indicated underneath each picture. In this example, maximal constriction, measured in response to 10^{-4} M of methacholine, was 63.5%.

Mouse	Saline					HDM				
	Sample size	Mean	SD	CoV	Median	Sample size	Mean	SD	CoV	Median
A. Airway constriction in lungs inflated by the traditional technique										
1	32	33.7	31.0	0.92	20.3	35	38.6	29.8	0.77	29.7
2	37	23.9	27.5	1.15	11.1	41	34.5	24.4	0.71	28.3
3	47	37.2	29.3	0.79	28.4	42	31.1	29.0	0.93	19.5
4	51	40.2	31.5	0.78	30.4	42	29.9	25.8	0.86	15.3
5	46	21.8	19.0	0.87	18.9	42	32.9	25.1	0.76	31.3
6	46	30.8	30.5	0.99	19.3	46	40.9	32.0	0.78	42.0
7	53	54.1	34.3	0.63	64.9	89	53.8	30.7	0.57	63.5
8	66	30.3	32.5	1.07	13.9	61	34.6	29.6	0.86	24.7
Average	47.3	34.0	29.4	0.90	25.9	49.8	37.0	28.3	0.78	31.8
B. Airway constriction in a lung lobe inflated by the needle technique										
1	41	38.0	38.5	1.01	23.5	35	38.0	33.6	0.88	22.6
2	36	24.2	30.2	1.25	9.3	40	53.1	36.5	0.69	52.6
3	39	32.3	34.1	1.06	10.4	39	35.6	31.7	0.89	27.7
4	37	24.8	25.4	1.03	15.0	41	32.3	28.7	0.89	29.0
5	31	37.1	34.2	0.92	33.0	42	55.9	28.1	0.50	64.3
6	41	28.8	31.6	1.10	12.3	38	37.3	30.2	0.81	40.6
7	46	50.2	33.9	0.67	57.8	57	38.1	33.6	0.88	25.0
8	63	47.2	34.0	0.72	48.2	55	29.8	31.9	1.07	18.0
Average	41.8	35.3	32.7	0.97	26.2	43.4	40.0	31.8	0.83	35.0

Table 1. Summary of data from mice exposed to either saline (left) or HDM (right) with their lung inflated with either the traditional technique (A) or the needle technique (B). Averages of the eight mice per subgroup are in bold. CoV, coefficient of variation; HDM, house-dust mite; SD, standard deviation.



Three-way ANOVA

Experimental asthma	0.85
Technique	0.89
Methacholine	<0.0001
Asthma x Technique	0.83
Asthma x Methacholine	0.003
Technique x Methacholine	0.58
Asthma x Technique x Methacholine	0.99

Fig. 2. Concentration–response curves, displaying airway constriction over increasing concentration of methacholine in mice exposed to either saline (blue) or house-dust mite (red) with their lungs inflated with either the traditional technique (darker colors) or with the needle technique (lighter colors). Results of the three-way ANOVA are shown below the graph. $n = 8$.

Simulations

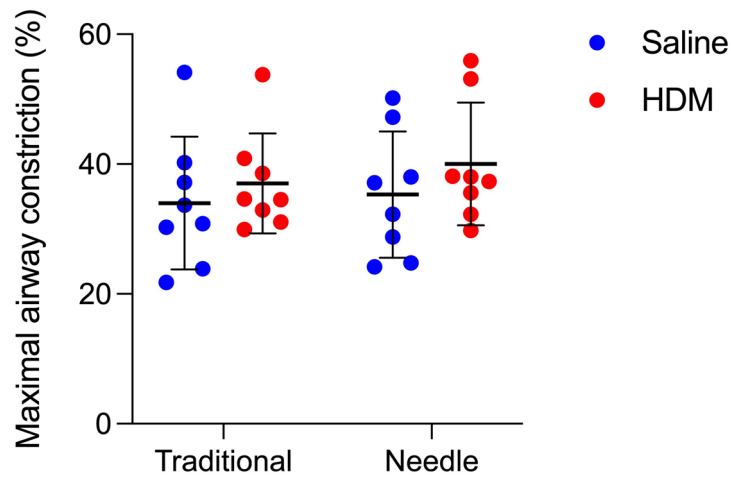
The minimum sample size to achieve reliable estimators (*i.e.*, mean, SD, CoV and median) of maximal constriction in each mouse is depicted in Table 2. As illustrated in Fig. 5, this value represents the minimum sample size where the running estimator would stabilize within a tolerance interval of $\pm 20\%$ of the final running estimator ($n = 150$) with 80% conformity. Further explanations are provided in Methods.

The minimum sample size varied between mice. For the 32 mice combined, the average minimum sample size is: 35 ± 10 for the mean, with a spread of 13–56; 16 ± 7 for the SD, with a spread of 9–41; and 29 ± 5 for the CoV, with a spread of 18–41. It can thus be seen that the minimum sample size also varied markedly between estimators (*i.e.*, mean, SD, CoV and median). In each subgroup, the SD exhibited the lowest minimum sample size, followed in order by the CoV, the mean and the median. In fact, the median never achieved stability within the set $\pm 20\%$ interval of tolerance for many mice over the sample sizes investigated (Table 2).

The minimum sample size also varies between subgroups. Experimental asthma significantly decreased the minimum sample size for the mean ($p = 0.021$), but not for the SD ($p = 0.43$) and the CoV ($p = 0.46$). In contrast, the inflating technique did not influence the minimum sample size for the mean ($p = 0.34$), the SD ($p = 0.46$) and the CoV ($p = 0.15$).

Table 2 also depicts this minimum sample size using intervals of tolerance of ± 10 or 5%. It can be seen that a greater accuracy quickly translates into substantially higher minimum sample sizes for all estimators. The change in the percentage of conformity with an increasing sample size is also depicted in Fig. 6. It is shown for each estimator and for every tested interval of tolerance in each subgroup of mice.

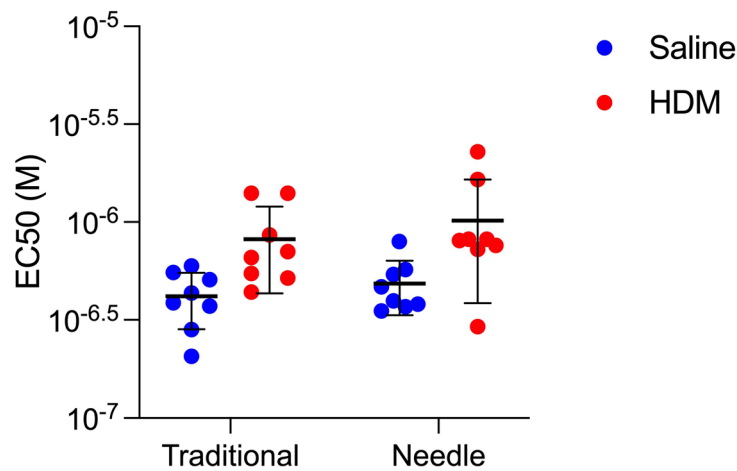
Finally, running the simulations again by analyzing only airways with baseline diameter between 150 and 350 μm did not significantly affect the minimum sample sizes. For the 32 mice combined and using an interval of tolerance of $\pm 20\%$ with 80% conformity, the average minimum sample size was then 34 ± 13 for the mean, 17 ± 11 for the SD, and 29 ± 5 for the CoV.



Two-way ANOVA

Experimental asthma	0.21
Technique	0.52
Interaction	0.83

Fig. 3. Maximal airway constriction, showing the constriction in response to the highest concentration of methacholine tested (*i.e.*, 10^{-4} M) in mice exposed to either saline (blue) or house-dust mite (red) with their lungs inflated with either the traditional technique or with the needle technique. Results of the two-way ANOVA are shown below the graph. n = 8.



Two-way ANOVA

Experimental asthma	0.002
Technique	0.33
Interaction	0.62

Fig. 4. The EC50, showing the concentration of methacholine causing 50% of the maximal response in mice exposed to either saline (blue) or house-dust mite (red) with their lungs inflated with either the traditional technique or with the needle technique. Results of the two-way ANOVA are shown below the graph. n = 8.

A. Mice exposed to saline with lungs inflated by the traditional technique.

Mouse	Tolerance \pm 20%				Tolerance \pm 10%				Tolerance \pm 5%			
	Mean	SD	CoV	Median	Mean	SD	CoV	Median	Mean	SD	CoV	Median
1	40	12	28	>125	87	35	70	>125	>125	79	116	>125
2	52	30	22	70	103	74	59	>125	>125	118	108	>125
3	30	14	28	105	75	42	71	>125	120	91	117	>125
4	31	13	23	116	76	37	64	>125	121	86	111	>125
5	36	15	28	113	83	45	74	>125	125	92	118	>125
6	42	15	33	>125	91	43	80	>125	>125	89	121	>125
7	21	10	35	66	58	28	82	120	106	70	123	>125
8	50	16	29	103	99	46	73	>125	>125	94	116	>125
Average	37.8	15.6	28.3		84	43.8	71.6			89.9	116.3	

B. Mice exposed to saline with a lung lobe inflated by the needle technique.

Mouse	Tolerance \pm 20%				Tolerance \pm 10%				Tolerance \pm 5%			
	Mean	SD	CoV	Median	Mean	SD	CoV	Median	Mean	SD	CoV	Median
1	46	13	30	>125	95	40	78	>125	>125	89	120	>125
2	56	33	25	90	106	77	64	>125	>125	119	112	>125
3	48	13	29	>125	98	40	73	>125	>125	88	118	>125
4	44	41	26	97	95	92	65	>125	>125	>125	112	>125
5	38	10	34	>125	86	28	83	>125	>125	69	123	>125
6	49	23	24	123	99	62	63	>125	>125	110	111	>125
7	24	9	34	110	62	24	79	>125	111	61	122	>125
8	27	11	31	82	73	30	77	>125	117	74	121	>125
Average	41.5	19.1	29.1		89.3	49.1	72.8				117.4	

C. Mice exposed to house-dust mite (HDM) with lungs inflated by the traditional technique.

Mouse	Tolerance \pm 20%				Tolerance \pm 10%				Tolerance \pm 5%			
	Mean	SD	CoV	Median	Mean	SD	CoV	Median	Mean	SD	CoV	Median
1	28	21	18	61	71	57	49	122	119	107	99	>125
2	26	11	26	>125	69	30	70	>125	117	76	117	>125
3	40	19	28	103	90	53	73	>125	>125	101	116	>125
4	34	10	28	>125	82	29	70	>125	125	69	119	>125
5	28	16	28	41	74	47	72	96	119	94	116	>125
6	31	10	33	>125	77	28	79	>125	120	67	122	>125
7	17	14	38	29	51	42	85	85	102	89	>125	>125
8	34	19	24	91	84	53	64	116	122	102	113	>125
Average	29.8	15	27.9		74.8	42.4	70.3			88.1		

D. Mice exposed to house-dust mite (HDM) with a lung lobe inflated by the needle technique.

Mouse	Tolerance \pm 20%				Tolerance \pm 10%				Tolerance \pm 5%			
	Mean	SD	CoV	Median	Mean	SD	CoV	Median	Mean	SD	CoV	Median
1	38	12	32	>125	84	34	76	>125	125	81	120	>125
2	24	10	29	108	65	26	74	>125	112	64	120	>125
3	35	15	26	119	85	47	68	>125	>125	97	114	>125
4	38	23	31	48	85	59	74	95	>125	108	118	>125
5	13	21	41	16	41	59	91	71	92	103	>125	>125
6	31	14	39	52	76	41	85	114	122	89	125	>125
7	37	10	31	>125	85	32	76	>125	125	75	119	>125
8	45	19	28	113	100	56	70	>125	>125	106	117	>125
Average	32.6	15.5	32.1		77.6	44.3	76.8			90.4		

Table 2. Summary of simulated data for mice of each subgroup (A through D). Averages of the eight mice per subgroup are in bold. The value in each cell represents the sample size required to achieve the indicated level of tolerance with **80% conformity** in terms of maximal constriction (*i.e.*, induced by 10^{-4} M of methacholine). This value is provided for the mean, the standard deviation (SD), the coefficient of variation (CoV) and the median in each mouse. The average of the eight mice is also provided on the last row if a value ≤ 125 was obtained for all mice.

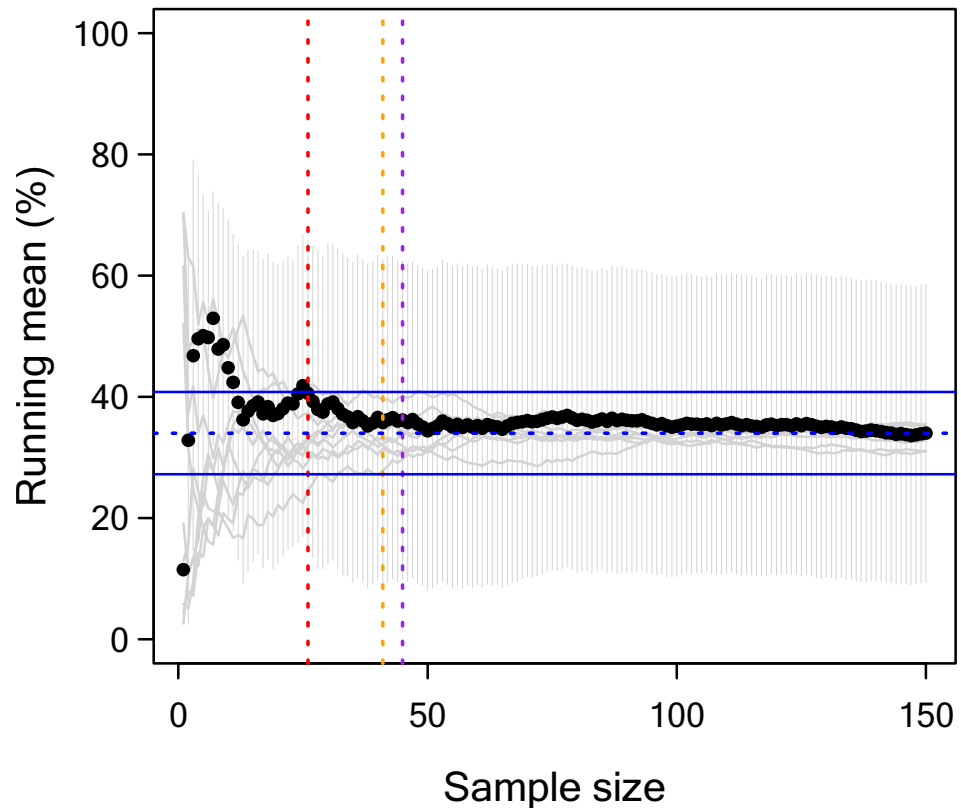


Fig. 5. A representative trace of one iteration (black dots), showing the evolution of the running mean for the maximal airway constriction over 150 samples selected randomly from the dataset of one mouse (mouse 2, exposed to house-dust mite and with its lungs inflated with the traditional technique). The vertical light gray bars are the standard deviation for this specific iteration. Nine other traces are also shown in gray in the background. The blue horizontal dotted line is a landmark showing the final running mean (*i.e.*, the running mean at $n = 150$). The blue lines in parallel represent the interval of tolerance, which was set in this example to be 20% above and below the final running mean. The red vertical dotted line is the point of stability, representing the minimum sample size ($n = 26$) for this specific iteration (in black) where all the subsequent running means never deviated from the final running mean by more than 20%. The orange and purple vertical dotted lines are landmarks showing the number of airways that were actually analyzed in this specific mouse ($n = 41$) and the average number of airways analyzed per mouse in this study ($n = 45$), respectively.

Discussion

Overall

In this study, the physioLens was used to measure airway constriction in response to six incremental concentrations of methacholine. It was done on an average of 45 ± 12 airways per mouse in 32 mice divided in four subgroups depending on their previous exposure to either saline or HDM and on whether their lungs had been inflated with the traditional or the needle technique. It is shown that experimental asthma, but not the inflating technique, significantly interacts with the response to methacholine. This interactive effect of experimental asthma was especially characterized by a decreased sensitivity to methacholine. Random sampling simulations then suggested that approximately 35, 16 and 29 airways would be the minimum sample sizes to assign a reliable mean, SD and CoV, respectively, of maximal constriction in one mouse.

Airway constriction in lung slices

Dandurand and coworkers were the first to study airway constriction in lung slices¹. Following technical refinements for cutting the lungs into slices from other pioneering work of Martin and coworkers⁷, the technique became commonly referred to as the precision-cut lung slice (PCLS). Although full of promise, studying airway constriction in lung slices entails dealing with an inconveniently large degree of variability^{1,3,4,6–38}. Indeed, in any given mouse, while an airway may constrict by 100%, another one may not budge in response to the same concentration of methacholine. One way of dealing with this variability is to increase the sample size. This is the strategy that was utilized in the present study. Using the physioLens, constriction was first quantified in 1457 airways in slices of lungs inflated by two different techniques from mice with or without experimental asthma. This collection of data was then used in simulation studies to determine the minimum sample size that would have been needed in each mouse in order to obtain a reliable value of airway constriction, as well as to determine the extent to which this minimum sample size varies between mice and between different experimental conditions.

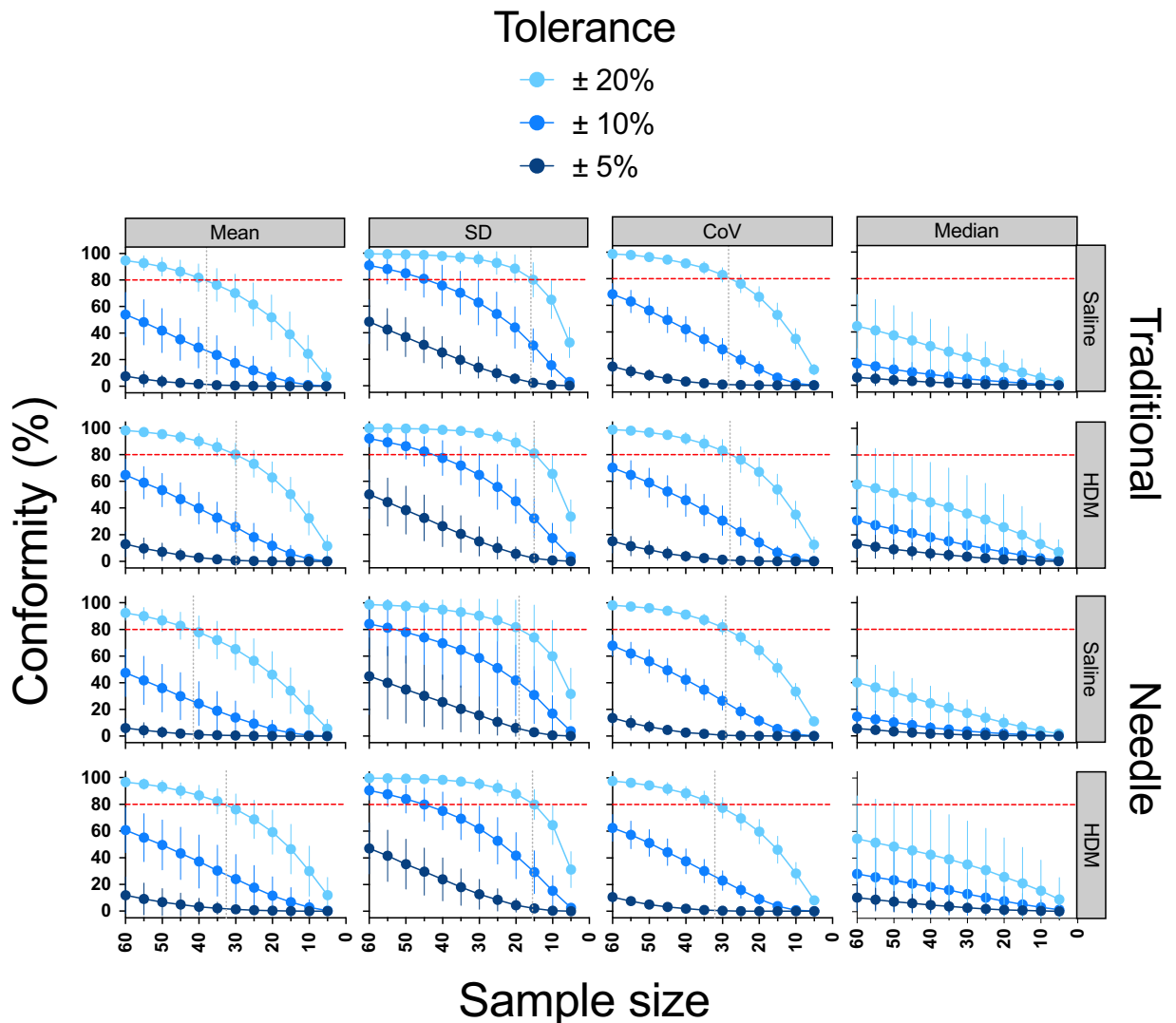


Fig. 6. Conformity over the sample size, showing how the percentage of conformity increases with increasing sample size at three different intervals of tolerance for each estimator (mean, SD, Coefficient of variation (CoV), and median) in each subgroup of mice. Every data point represents the mean \pm SD of 8 mice. For clarity, only results of every fifth sample size are shown. The red horizontal dotted line in every graph is the set level of conformity used in the present study. The gray vertical dotted line in some graphs is aligned with the sample size where 80% conformity was achieved when the interval of tolerance was set at $\pm 20\%$. These latter sample sizes are also shown as the average of every subgroup of mice for each estimator in Table 2.

Minimum number of airways to analyze per mouse

These simulation studies were an attempt to guide future experimenters regarding the minimum sample size that is required to obtain a reliable value per mouse for each estimator of airway constriction. The chosen interval of tolerance (i.e., $\pm 20\%$) and the accepted percentage of conformity (i.e., 80%) were arbitrary and can be tailored to any desired level of accuracy depending on the purpose. It was still concluded that owing to the inherently large variability of airway constriction in lung slices, varying from nil to 100%, the median will never be a practical estimator of central dispersion. Inversely, the variability within each mouse (SD and CoV) stabilized at relatively low sample sizes, meaning that in instances where the objective is to capture heterogeneity, lower sample sizes (16 ± 7 for the SD and 29 ± 5 for the CoV) should normally be enough. Finally, the minimum sample size to obtain a reliable mean stabilized at intermediate numbers of 35 ± 10 airways.

The minimum sample size for each estimator varied substantially between mice. Although some of this inter-subject variability may be biological, we think a lot of it can also be related to other technical issues, such as barotrauma or insufficient inflation in part of the lungs, variable degree of damage during slicing, changing agarose temperature across the lung during filling, etc. Other solutions will need to be advanced to address these potential sources of variability.

Experimental asthma on airway constriction

The minimum sample sizes were on average smaller in mice exposed to HDM *versus* saline (Table 2). The reason for this is unfortunately unclear. Experimental asthma also significantly interacts with airway constriction induced by incremental concentrations of methacholine (Fig. 2). The concentration–response curves in experimental asthma were indeed shifted. Further analyses suggested that while maximal constriction was not affected significantly by experimental asthma (Fig. 3), the sensitivity to methacholine was significantly decreased (Fig. 4). It is thus concluded that the main effect of experimental asthma is to decrease the sensitivity to methacholine, at least in the mouse model of asthma used herein. This could have not been predicted based on a previous study, showing no differences in tracheal contractility between mice with and without experimental asthma using the same model and the same strain of mice³⁹. Nonetheless, the decreased sensitivity of the airway smooth muscle to methacholine in asthma was reported previously by many others^{40–46}.

More studies will obviously be needed to test the sensitivity of airways in lung slices from other animal models of asthma, as well as in asthmatic individuals. In other studies on lung slices in mouse models of asthma, a decrease²², no changes^{23,47}, or an increase²⁴ in airway constriction to methacholine was reported. Importantly, no enlargement of the airway smooth muscle is observed in the asthma model used in the present study^{39,48}. Other studies using different models have shown varying degrees of airway smooth muscle remodeling, as well as other structural changes in the airway wall and the parenchyma, such as collagen deposition, which may perhaps explain some discrepancies^{22–24}. Notably, mouse strains and sex also greatly influence the response to methacholine^{49,50}. Future studies will be needed to isolate the effect of each of these confounders on airway constriction in lung slices.

In combination with previous findings, the present study also provides important insights about the root cause of hyperresponsiveness. Using the same model of asthma and the same mouse strain, it was clearly shown that mice with experimental asthma exhibits hyperresponsiveness to nebulized methacholine *in vivo*^{39,48}. As aforementioned, the contractility of the excised trachea between mice with and without experimental asthma was also measured in one of the latter studies in order to compare isometric force, a widely used readout to assess the contractile capacity of the airway smooth muscle. Isometric force was shown to be virtually identical between mice with and without experimental asthma³⁹. It was concluded that defects in smooth muscle contractility are unlikely to contribute to *in vivo* hyperresponsiveness in this specific mouse model. Yet, isometric force does not occur *in vivo* and may not be the best contractile readout to assess the muscle's contribution to the *in vivo* response to methacholine⁵¹. *Ex vivo* isometric force actually correlates very poorly with the level of *in vivo* response to methacholine in both mice⁵² and humans^{45,53–59}. Inasmuch as the lung slice technique is a proper *ex vivo* model for quantifying airway constriction, the present study suggests that excessive airway narrowing due to exaggerated airway smooth muscle shortening is also not a feature contributing to methacholine hyperresponsiveness *in vivo* in this specific mouse model of asthma. These findings are thus more consistent with a mounting literature, suggesting that the root cause of hyperresponsiveness in asthma or experimental asthma is not due to a defect in airway smooth muscle contraction but to airway narrowing heterogeneity^{60–66} and closure^{60,67–69}.

Inflating technique on airway constriction

The inflating technique had no significant effect on the minimum sample size for any of the estimators. Additionally, the choice of inflating technique neither affected airway constriction nor the effect of experimental asthma on the methacholine response. This is convenient. It means that the lungs can either be inflated by infusing agarose into the trachea when the whole lungs are available or by injecting several boluses of agarose with a needle in an excised lobe without significantly changing the outcomes. Since the former technique is most commonly employed with animal tissues and the latter with human tissues, the lack of differences between the two techniques in the same tissue reinforces the translatability of animal work. Obviously, this finding does not obviate the need to compare with a piece of lung with wide perforations of its visceral pleura (*vs.* the several needle-wide perforations used in the present study), which is most often the case with human tissues. The inflation with the needle in an excised lobe may also be advantageous because it implies that the other lobes would be available for other purposes. In line with the 3Rs, this would limit the number of animals in research.

Conclusion

The large variability of airway constriction in lung slices implies studying large sample sizes, which come with practical difficulties. Herein, the physioLens was used to unbiasedly quantify airway constriction in a great number of airways in a fully automated manner. The approach was successful to measure airway constrictions in lungs from mice with and without experimental asthma that were inflated by two different techniques. It is predicted that analyzing approximately 35, 16 and 29 airways would provide a reliable mean, SD and CoV, respectively, of maximal constriction in one mouse. Although these numbers vary from mouse to mouse and between mice with and without experimental asthma, we hope it will provide guidance for future experimenters regarding the minimum sample size that is required per mouse to obtain estimators of contraction that suited any desired level of accuracy.

Methods

Mice

Thirty-two male BALB/c mice (Charles River, Saint-Constant, Canada) were studied at 9–11 weeks of age. They were provided food and water *ad libitum* at all times. All methods were approved by the Committee of Animal Care of *Université Laval* following the guidelines from the Canadian Council on Animal Care (protocol 2023–1303-1) and complied with the ARRIVE guidelines.

Experimental asthma

Half of mice were exposed to 25 μL of saline and the other half to 25 μL of 2 mg/mL of house-dust mite (HDM) extract (*D. pteronyssinus*, lot number 360923; Greer, Lenoir, NC) diluted in saline to induce pulmonary allergic inflammation^{39,70,71}. The endotoxin concentration was 47.3 EU per mg of HDM extract. They were exposed through an intranasal instillation once daily under isoflurane anesthesia for 10 consecutive days. All outcomes were measured 24 h after the last exposure.

Lung slices

Mice were euthanized with an overdose of ketamine (300 mg/kg) and xylazine (30 mg/kg) injected intraperitoneally. Thoracotomy was performed and the chest was opened. Two common techniques were used to fill and inflate the lungs with agarose (Bio-Rad Laboratories, cat #1613112, Redmond, WA, USA). Each group (saline- and HDM-exposed mice) was thus divided into two subgroups, ending with eight mice in each of the four subgroups. The first inflation technique was the single intratracheal infusion, called the traditional technique. The second inflation technique was several injections through the parenchyma with a needle, called the needle technique. For the traditional technique, while the lungs were still resting inside the thorax, a tracheotomy was performed and 1.1–1.2 mL of agarose pre-warmed at 40 °C was infused into the lungs through the trachea using an 18-gauge syringe. For the needle technique, the left lung, which is a lung with a single lobe in mice, was first excised and then inflated with the same agarose but by injecting several boluses within the parenchyma (across the visceral pleura) at various locations using a 27-gauge syringe until the entire lung was clearly bulged. After inflation for both techniques, the lungs were plunged into ice-cold Hank's balanced salt solution (HBSS) for 30 min to polymerize the agarose. The left lobe was subsequently cut into 200- μm slices in the sagittal orientation using the Compresstome VF-310 (Precisionary Instruments, Ashland, MA, USA). Slices were more precisely selected in the middle part of the lobe, avoiding the first and last 20% edges. Finally, the lung slices were immersed in Dulbecco's Modified Eagle's Medium (DMEM) supplemented with 1% penicillin, streptomycin and amphotericin B into a 6-well plate and kept at 37 °C for 24 h. Two to three slices were inserted in each well.

Airway constriction

The first step consisted of removing the DMEM and washing the slices twice with warm HBSS. The slices were then fixed in the middle of the well with SCIREQ slice holders (physioMesh) in 6 mL of warm HBSS, and subsequently transferred to the physioLens (SCIREQ, Montreal, Canada; <https://www.scireq.com/physiolens/>). The experimenter selected on the computer screen all clearly visible airways with a perpendicular orientation in relation to the field of view (*i.e.*, circular airways), with no apparent damages, and with clear cilia beating. The algorithm to determine the contour is done in the following steps.

- Pre-processing by morphological operation to remove small items or noise.
- Converting the images to binary.
- Running an edge detection algorithm.
- Using a contour detection algorithm on the edges.
- With this contour, the area of the airway is found.

The x , y and z positions of airways are also recorded by the software, which are subsequently used to track luminal narrowing over time during the constriction assay. The physioLens is also equipped with a robotized eight-fluid handling system, allowing the pre-programming of hours-long, fully automated protocols.

The following steps are thus performed automatically by the physioLens, one well at the time. The lung slice is first washed again with HBSS and left untouched for 4 min. The washing step is done with a two-nozzle system. The two nozzles are positioned on opposite poles along the perimeter of the well. One infuses the fluid and the other aspirates it, causing a swirling movement of the fluid in the well without displacing the slice. The flow (2.3 mL/s) in the infusing nozzle was selected so that at least 95% replacement of the fluid is completed in less than 20 s. This first washing step also allows many airways to fully dilate. The constricting assay is then started automatically. The smooth muscle was stimulated to contract with methacholine dissolved in 37 °C-warmed HBSS at six incremental concentrations, namely 5×10^{-8} , 10^{-7} , 5×10^{-7} , 10^{-6} , 10^{-5} and 10^{-4} M. Each concentration was substituted at 4 min intervals, as explained above for the washing step. Images of luminal area were collected in all pre-selected airways within the well every min. Constriction, expressed in percentage of decrease in relation to the initial luminal area (the one at the end of the washing step with HBSS), is also calculated automatically with the physioLens. The maximal constriction obtained during the 4 min of recording at every methacholine concentration was used to generate the concentration–response curve. An example of a constricting airway is shown in Fig. 1.

Statistics

Unless otherwise indicated, data are presented as means \pm SD. The constriction of all airways in each mouse at every methacholine concentration was first averaged to obtain one value of constriction per concentration per mouse. Since data of constriction are in percentage, they were first log-transformed prior to statistical analysis. A three-way $2 \times 2 \times 6$ ANOVAs was then used to measure the effect of experimental asthma (saline- vs. HDM-exposed mice), the inflating technique (traditional vs. needle) and the concentrations of methacholine (6 concentrations) on airway constriction, as well as their interactions. It was followed by Tukey's multiple comparisons test to compare, in a pairwise fashion, between subgroups at every methacholine concentration. The EC50 (*i.e.*, the concentration causing 50% of the maximal response) was also calculated in each mouse by fitting

a concentration–response curve with four parameters (top, bottom, EC50, and Hill slope). Two-way ANOVAs were also used to investigate the effect of experimental asthma, the inflating technique, and their interaction on baseline airway caliber, the EC50 and the maximal response (*i.e.*, the constriction at the highest methacholine concentration tested). All statistical analyses were performed using Prism 10 (version 10.2.1, GraphPad, San Diego, CA). $P < 0.05$ was considered statistically significant.

Random sampling simulations

The number of airways that need to be sampled to obtain a reliable estimate of the mean, SD, CoV, and median in each mouse is unknown. Using our dataset, simulation studies were conducted to predict a minimum sample size for reliably estimating maximal constriction (*i.e.*, the one induced by 10^{-4} M of methacholine). The method was inspired by others^{72,73}.

From the dataset of each mouse ($n = 31–89$), 150 samples were sequentially drawn randomly with replacement. Each of the running estimators (mean, SD, CoV and median) was calculated after each draw and the sample size at which the running estimator settled within a tolerance interval between $\pm 20\%$ of the final running estimator (*i.e.*, the running estimator at the 150th sample) was identified. This sample size represents the point of stability, where all the subsequent running estimators never go below or above the set interval of tolerance (meaning that from this point and onwards, the experimenter would be analyzing more airways without substantially affecting the average of its estimators). An example for the mean is depicted in Fig. 5. This process was iterated 1000 times and, at each running sample size, the number of iterations in which all the subsequent running estimators were within the set interval of tolerance was counted to calculate the percentage of conformity. An 80% conformity, for example, means that for 800 of the 1000 iterations, all the subsequent running estimators beyond the sample size investigated were within the set interval of tolerance. In the present study, the sample size where 80% conformity was attained was considered the minimum sample size to provide a reliable value of an estimator. For future experimenters who would require a greater level of accuracy, minimum sample sizes for each estimator were also recalculated at two narrower intervals of tolerance, namely ± 10 and 5%, using the same level of conformity (80%). Finally, the simulations were run again using only airways with a baseline airway diameter between 150 and 350 μm . The goal was to assess whether removing the very small and very large airways would change the minimum sample sizes. The number of airways analyzed per mouse was then on average 34.3 with a SD of ± 10.2 and a spread of 22–66.

Data availability

The datasets used and analyzed during the current study are available from the corresponding author on reasonable request.

Received: 10 May 2024; Accepted: 26 August 2024

Published online: 29 August 2024

References

- Dandurand, R. J., Wang, C. G., Phillips, N. C. & Eidelman, D. H. Responsiveness of individual airways to methacholine in adult rat lung explants. *J. Appl. Physiol.* **1985**(75), 364–372. <https://doi.org/10.1152/jappl.1993.75.1.364> (1993).
- Rosner, S. R. *et al.* Airway contractility in the precision-cut lung slice after cryopreservation. *Am. J. Respir. Cell Mol. Biol.* **50**, 876–881. <https://doi.org/10.1165/rcmb.2013-0166MA> (2014).
- Struckmann, N. *et al.* Role of muscarinic receptor subtypes in the constriction of peripheral airways: Studies on receptor-deficient mice. *Mol. Pharmacol.* **64**, 1444–1451. <https://doi.org/10.1124/mol.64.6.1444> (2003).
- Yang, Z. *et al.* Beta-agonist-associated reduction in RGS5 expression promotes airway smooth muscle hyper-responsiveness. *J. Biol. Chem.* **286**, 11444–11455. <https://doi.org/10.1074/jbc.M110.212480> (2011).
- Van Dijk, E. M., Culha, S., Menzen, M. H., Bidan, C. M. & Gosens, R. Elastase-induced parenchymal disruption and airway hyper-responsiveness in mouse precision cut lung slices: Toward an ex vivo COPD model. *Front. Physiol.* **7**, 657. <https://doi.org/10.3389/fphys.2016.00657> (2016).
- Balenga, N. A. *et al.* A fungal protease allergen provokes airway hyper-responsiveness in asthma. *Nat. Commun.* **6**, 6763. <https://doi.org/10.1038/ncomms7763> (2015).
- Martin, C., Uhlig, S. & Ullrich, V. Videomicroscopy of methacholine-induced contraction of individual airways in precision-cut lung slices. *Eur. Respir. J.* **9**, 2479–2487. <https://doi.org/10.1183/09031936.96.09122479> (1996).
- Maarsingh, H. *et al.* Small airway hyperresponsiveness in COPD: Relationship between structure and function in lung slices. *Am. J. Physiol. Lung Cell. Mol. Physiol.* **316**, L537–L546. <https://doi.org/10.1152/ajplung.00325.2018> (2019).
- Donovan, C., Royce, S. G., Vlahos, R. & Bourke, J. E. Lipopolysaccharide does not alter small airway reactivity in mouse lung slices. *PLoS One* **10**, e0122069. <https://doi.org/10.1371/journal.pone.0122069> (2015).
- Parikh, V. *et al.* Rhinovirus C15 induces airway hyperresponsiveness via calcium mobilization in airway smooth muscle. *Am. J. Respir. Cell Mol. Biol.* **62**, 310–318. <https://doi.org/10.1165/rcmb.2019-0004OC> (2020).
- Chen, J. *et al.* Orosomucoid-like 3 (ORMDL3) upregulates airway smooth muscle proliferation, contraction, and Ca(2+) oscillations in asthma. *J. Allergy Clin. Immunol.* **142**, 207–218. <https://doi.org/10.1016/j.jaci.2017.08.015> (2018).
- Rosner, S. R. *et al.* The actin regulator zyxin reinforces airway smooth muscle and accumulates in airways of fatal asthmatics. *PLoS One* **12**, e0171728. <https://doi.org/10.1371/journal.pone.0171728> (2017).
- Cook, D. P. *et al.* Cystic fibrosis transmembrane conductance regulator in sarcoplasmic reticulum of airway smooth muscle. Implications for airway contractility. *Am. J. Respir. Crit. Care Med.* **193**, 417–426. <https://doi.org/10.1164/rccm.201508-1562OC> (2016).
- Kistemaker, L. E. M. *et al.* The PDE4 inhibitor CHF-6001 and LAMAs inhibit bronchoconstriction-induced remodeling in lung slices. *Am. J. Physiol. Lung Cell. Mol. Physiol.* **313**, L507–L515. <https://doi.org/10.1152/ajplung.00069.2017> (2017).
- Martin, C., Ullrich, V. & Uhlig, S. Effects of the thromboxane receptor agonist U46619 and endothelin-1 on large and small airways. *Eur. Respir. J.* **16**, 316–323 (2000).
- Donovan, C., Seow, H. J., Bourke, J. E. & Vlahos, R. Influenza A virus infection and cigarette smoke impair bronchodilator responsiveness to beta-adrenoceptor agonists in mouse lung. *Clin. Sci. (Lond)* **130**, 829–837. <https://doi.org/10.1042/CS20160093> (2016).

17. van den Berg, M. P. M. *et al.* The novel TRPA1 antagonist BI01305834 inhibits ovalbumin-induced bronchoconstriction in guinea pigs. *Respir. Res.* **22**, 48. <https://doi.org/10.1186/s12931-021-01638-7> (2021).
18. Zuo, H. *et al.* Cigarette smoke up-regulates PDE3 and PDE4 to decrease cAMP in airway cells. *Br. J. Pharmacol.* **175**, 2988–3006. <https://doi.org/10.1111/bph.14347> (2018).
19. Tigges, J., Worek, F., Thiermann, H. & Wille, T. Organophosphorus pesticides exhibit compound specific effects in rat precision-cut lung slices (PCLS): Mechanisms involved in airway response, cytotoxicity, inflammatory activation and antioxidative defense. *Arch. Toxicol.* <https://doi.org/10.1007/s00204-021-03186-x> (2021).
20. Kennedy, J. L. *et al.* Effects of rhinovirus 39 infection on airway hyperresponsiveness to carbachol in human airways precision cut lung slices. *J. Allergy Clin. Immunol.* **141**, 1887–1890. <https://doi.org/10.1016/j.jaci.2017.11.041> (2018).
21. Zeng, Z. *et al.* Inherent differences of small airway contraction and Ca(2+) oscillations in airway smooth muscle cells between BALB/c and C57BL/6 mouse strains. *Front. Cell Dev. Biol.* **11**, 1202573. <https://doi.org/10.3389/fcell.2023.1202573> (2023).
22. Donovan, C. *et al.* Differential effects of allergen challenge on large and small airway reactivity in mice. *PLoS One* **8**, e74101. <https://doi.org/10.1371/journal.pone.0074101> (2013).
23. Kim, H. J. *et al.* Airway smooth muscle sensitivity to methacholine in precision-cut lung slices (PCLS) from ovalbumin-induced asthmatic mice. *Korean J. Physiol. Pharmacol.* **19**, 65–71. <https://doi.org/10.4196/kjpp.2015.19.1.65> (2015).
24. Liu, G. *et al.* Airway remodelling and inflammation in asthma are dependent on the extracellular matrix protein fibulin-1c. *J. Pathol.* **243**, 510–523. <https://doi.org/10.1002/path.4979> (2017).
25. Yocum, G. T. *et al.* Role of transient receptor potential vanilloid 1 in the modulation of airway smooth muscle tone and calcium handling. *Am. J. Physiol. Lung Cell. Mol. Physiol.* **312**, L812–L821. <https://doi.org/10.1152/ajplung.00064.2017> (2017).
26. Chen, J. & Sanderson, M. J. Store-operated calcium entry is required for sustained contraction and Ca(2+) oscillations of airway smooth muscle. *J. Physiol.* **595**, 3203–3218. <https://doi.org/10.1113/JP272694> (2017).
27. Bergner, A. & Sanderson, M. J. Acetylcholine-induced calcium signaling and contraction of airway smooth muscle cells in lung slices. *J. Gen. Physiol.* **119**, 187–198. <https://doi.org/10.1085/jgp.119.2.187> (2002).
28. Perez, J. F. & Sanderson, M. J. The frequency of calcium oscillations induced by 5-HT, ACH, and KCl determine the contraction of smooth muscle cells of intrapulmonary bronchioles. *J. Gen. Physiol.* **125**, 535–553. <https://doi.org/10.1085/jgp.200409216> (2005).
29. Bai, Y., Zhang, M. & Sanderson, M. J. Contractility and Ca2+ signaling of smooth muscle cells in different generations of mouse airways. *Am. J. Respir. Cell Mol. Biol.* **36**, 122–130. <https://doi.org/10.1165/rcmb.2006-0036OC> (2007).
30. Perez-Zoghbi, J. F. & Sanderson, M. J. Endothelin-induced contraction of bronchiole and pulmonary arteriole smooth muscle cells is regulated by intracellular Ca2+ oscillations and Ca2+ sensitization. *Am. J. Physiol. Lung Cell. Mol. Physiol.* **293**, L1000–L1011. <https://doi.org/10.1152/ajplung.00184.2007> (2007).
31. Bergner, A. & Sanderson, M. J. Airway contractility and smooth muscle Ca(2+) signaling in lung slices from different mouse strains. *J. Appl. Physiol.* **1985**(95), 1325–1332. <https://doi.org/10.1152/jappphysiol.00272.2003> (2003).
32. Bai, Y. *et al.* Cryopreserved human precision-cut lung slices as a bioassay for live tissue banking. A viability study of bronchodilation with bitter-taste receptor agonists. *Am. J. Respir. Cell Mol. Biol.* **54**, 656–663. <https://doi.org/10.1165/rcmb.2015-0290MA> (2016).
33. Bourke, J. E. *et al.* Novel small airway bronchodilator responses to rosiglitazone in mouse lung slices. *Am. J. Respir. Cell Mol. Biol.* **50**, 748–756. <https://doi.org/10.1165/rcmb.2013-0247OC> (2014).
34. Donovan, C. *et al.* Rosiglitazone is a superior bronchodilator compared to chloroquine and beta-adrenoceptor agonists in mouse lung slices. *Respir. Res.* **15**, 29. <https://doi.org/10.1186/1465-9921-15-29> (2014).
35. FitzPatrick, M., Donovan, C. & Bourke, J. E. Prostaglandin E2 elicits greater bronchodilation than salbutamol in mouse intrapulmonary airways in lung slices. *Pulm. Pharmacol. Ther.* **28**, 68–76. <https://doi.org/10.1016/j.pupt.2013.11.005> (2014).
36. Tan, X. & Sanderson, M. J. Bitter tasting compounds dilate airways by inhibiting airway smooth muscle calcium oscillations and calcium sensitivity. *Br. J. Pharmacol.* **171**, 646–662. <https://doi.org/10.1111/bph.12460> (2014).
37. Ma, B., Sanderson, M. & Bates, J. H. Airway-parenchymal interdependence in the lung slice. *Respir. Physiol. Neurobiol.* **185**, 211–216. <https://doi.org/10.1016/j.resp.2012.10.015> (2013).
38. Perez-Zoghbi, J. F., Bai, Y. & Sanderson, M. J. Nitric oxide induces airway smooth muscle cell relaxation by decreasing the frequency of agonist-induced Ca2+ oscillations. *J. Gen. Physiol.* **135**, 247–259. <https://doi.org/10.1085/jgp.200910365> (2010).
39. Boucher, M., Henry, C., Dufour-Mailhot, A., Khadangi, F. & Bossé, Y. Smooth muscle hypocontractility and airway normoresponsiveness in a mouse model of pulmonary allergic inflammation. *Front. Physiol.* **12**, 698019. <https://doi.org/10.3389/fphys.2021.698019> (2021).
40. Ijpma, G. *et al.* Intrapulmonary airway smooth muscle is hyperreactive with a distinct proteome in asthma. *Eur. Respir. J.* **56**, 1902178. <https://doi.org/10.1183/13993003.02178-2019> (2020).
41. Ijpma, G. *et al.* Human trachealis and main bronchi smooth muscle are normoresponsive in asthma. *Am. J. Respir. Crit. Care Med.* **191**, 884–893. <https://doi.org/10.1164/rccm.201407-1296OC> (2015).
42. Goldie, R. G., Spina, D., Henry, P. J., Lulich, K. M. & Paterson, J. W. In vitro responsiveness of human asthmatic bronchus to carbachol, histamine, beta-adrenoceptor agonists and theophylline. *Br. J. Clin. Pharmacol.* **22**, 669–676 (1986).
43. Bai, T. R. Abnormalities in airway smooth muscle in fatal asthma. *Am. Rev. Respir. Dis.* **141**, 552–557 (1990).
44. Bai, T. R. Abnormalities in airway smooth muscle in fatal asthma. A comparison between trachea and bronchus. *Am. Rev. Respir. Dis.* **143**, 441–443 (1991).
45. Whicker, S. D., Armour, C. L. & Black, J. L. Responsiveness of bronchial smooth muscle from asthmatic patients to relaxant and contractile agonists. *Pulm. Pharmacol.* **1**, 25–31 (1988).
46. Van Koppen, C. J. *et al.* Muscarinic receptor sensitivity in airway smooth muscle of patients with obstructive airway disease. *Arch. Int. Pharmacodyn. Ther.* **295**, 238–244 (1988).
47. Bourke, J. *et al.* The calcium-sensing receptor CaSR mediates airway contraction in a house dust mite model of allergic airway disease. *Eur. Respir. J.* **54**, PA3884. <https://doi.org/10.1183/13993003.congress-2019.PA3884> (2019).
48. Gill, R., Rojas-Ruiz, A., Boucher, M., Henry, C. & Bossé, Y. More airway smooth muscle in males versus females in a mouse model of asthma: A blessing in disguise? *Exp. Physiol.* **108**, 1080–1091. <https://doi.org/10.1113/EP091236> (2023).
49. Card, J. W. *et al.* Male sex hormones promote vagally mediated reflex airway responsiveness to cholinergic stimulation. *Am. J. Physiol. Lung Cell. Mol. Physiol.* **292**, L908–L914. <https://doi.org/10.1152/ajplung.00407.2006> (2007).
50. Boucher, M., Henry, C. & Bossé, Y. Force adaptation through the intravenous route in naive mice. *Exp. Lung Res.* **49**, 131–141. <https://doi.org/10.1080/01902148.2023.2237127> (2023).
51. Bossé, Y. & Paré, P. D. The contractile properties of airway smooth muscle: How their defects can be linked to asthmatic airway hyperresponsiveness? *Curr. Respir. Med. Rev.* **9**, 42–68 (2013).
52. Weinmann, G. G., Black, C. M., Levitt, R. C. & Hirshman, C. A. In vitro tracheal responses from mice chosen for in vivo lung cholinergic sensitivity. *J. Appl. Physiol.* **1985**(69), 274–280. <https://doi.org/10.1152/jappl.1990.69.1.274> (1990).
53. Armour, C. L., Black, J. L., Berend, N. & Woolcock, A. J. The relationship between bronchial hyperresponsiveness to methacholine and airway smooth muscle structure and reactivity. *Respir. Physiol.* **58**, 223–233 (1984).
54. Armour, C. L. *et al.* A comparison of in vivo and in vitro human airway reactivity to histamine. *Am. Rev. Respir. Dis.* **129**, 907–910 (1984).
55. Cerrina, J. *et al.* Comparison of human bronchial muscle responses to histamine in vivo with histamine and isoproterenol agonists in vitro. *Am. Rev. Respir. Dis.* **134**, 57–61 (1986).

56. Taylor, S. M., Pare, P. D., Armour, C. L., Hogg, J. C. & Schellenberg, R. R. Airway reactivity in chronic obstructive pulmonary disease. Failure of in vivo methacholine responsiveness to correlate with cholinergic, adrenergic, or nonadrenergic responses in vitro. *Am. Rev. Respir. Dis.* **132**, 30–35. <https://doi.org/10.1164/arrd.1985.132.1.30> (1985).
57. de Jongste, J. C. *et al.* Comparison of maximal bronchoconstriction in vivo and airway smooth muscle responses in vitro in non-asthmatic humans. *Am. Rev. Respir. Dis.* **138**, 321–326. <https://doi.org/10.1164/ajrccm/138.2.321> (1988).
58. Thomson, N. C. In vivo versus in vitro human airway responsiveness to different pharmacologic stimuli. *Am. Rev. Respir. Dis.* **136**, S58–S62. https://doi.org/10.1164/ajrccm/136.4_Pt_2.S58 (1987).
59. Roberts, J. A., Rodger, I. W. & Thomson, N. C. In vivo and in vitro human airway responsiveness to leukotriene D4 in patients without asthma. *J. Allergy Clin. Immunol.* **80**, 688–694. [https://doi.org/10.1016/0091-6749\(87\)90288-0](https://doi.org/10.1016/0091-6749(87)90288-0) (1987).
60. Dame Carroll, J. R., Magnussen, J. S., Berend, N., Salome, C. M. & King, G. G. Greater parallel heterogeneity of airway narrowing and airway closure in asthma measured by high-resolution CT. *Thorax* **70**, 1163–1170. <https://doi.org/10.1136/thoraxjnl-2014-206387> (2015).
61. Downie, S. R. *et al.* Ventilation heterogeneity is a major determinant of airway hyperresponsiveness in asthma, independent of airway inflammation. *Thorax* **62**, 684–689. <https://doi.org/10.1136/thx.2006.069682> (2007).
62. Farrow, C. E. *et al.* Peripheral ventilation heterogeneity determines the extent of bronchoconstriction in asthma. *J. Appl. Physiol.* **1985**(123), 1188–1194. <https://doi.org/10.1152/jappphysiol.00640.2016> (2017).
63. Hardaker, K. M. *et al.* Predictors of airway hyperresponsiveness differ between old and young patients with asthma. *Chest* **139**, 1395–1401. <https://doi.org/10.1378/chest.10-1839> (2011).
64. King, G. G. *et al.* Heterogeneity of narrowing in normal and asthmatic airways measured by HRCT. *Eur. Respir. J.* **24**, 211–218 (2004).
65. Lutchen, K. R., Hantos, Z., Petak, F., Adamicza, A. & Suki, B. Airway inhomogeneities contribute to apparent lung tissue mechanics during constriction. *J. Appl. Physiol.* **1985**(80), 1841–1849 (1996).
66. Petak, F., Hantos, Z., Adamicza, A., Asztalos, T. & Sly, P. D. Methacholine-induced bronchoconstriction in rats: Effects of intravenous vs. aerosol delivery. *J. Appl. Physiol.* **82**, 1479–1487. <https://doi.org/10.1152/jappl.1997.82.5.1479> (1997).
67. Chapman, D. G., Berend, N., King, G. G. & Salome, C. M. Increased airway closure is a determinant of airway hyperresponsiveness. *Eur. Respir. J.* **32**, 1563–1569 (2008).
68. Farrow, C. E. *et al.* Airway closure on imaging relates to airway hyperresponsiveness and peripheral airway disease in asthma. *J. Appl. Physiol.* **113**, 958–966. <https://doi.org/10.1152/jappphysiol.01618.2011> (2012).
69. Wagers, S., Lundblad, L. K., Ekman, M., Irvin, C. G. & Bates, J. H. The allergic mouse model of asthma: Normal smooth muscle in an abnormal lung? *J. Appl. Physiol.* **96**, 2019–2027 (2004).
70. Boucher, M., Henry, C., Khadangi, F., Dufour-Mailhot, A. & Bossé, Y. Double-chamber plethysmography versus oscillometry to detect baseline airflow obstruction in a model of asthma in two mouse strains. *Exp. Lung Res.* **47**, 390–401. <https://doi.org/10.1080/01902148.2021.1979693> (2021).
71. Sahu, N., Morales, J. L., Fowell, D. & August, A. Modeling susceptibility versus resistance in allergic airway disease reveals regulation by Tec kinase Itk. *PLoS One* **5**, e11348. <https://doi.org/10.1371/journal.pone.0011348> (2010).
72. Hammer, N. *et al.* Sample size considerations in soft tissue biomechanics. *Acta Biomater.* **169**, 168–178. <https://doi.org/10.1016/j.actbio.2023.07.036> (2023).
73. Schönbrodt, F. D. & Perugini, M. At what sample size do correlations stabilize?. *J. Res. Pers.* **47**, 609–612 (2013).

Author contributions

All authors edited the manuscript, and read and approved the final manuscript. M.B., C.H., L.F., P.G. and Y.B. contributed to the development of the experimental design. M.B., L.G., R.P. and A.R.R. performed laboratory experiments. M.B. and Y.B. analyzed the data. Y.B. wrote the manuscript.

Funding

Natural Sciences and Engineering Research Council of Canada (NSERC) in partnership with SCIREQ (ALLRP-570485-2021 & RGPIN-2020-06355), the Canadian Institutes of Health Research (CIHR, 508356-202209PJT); and the Fondation de l'UCPQ (*Institut Universitaire de Cardiologie et de Pneumologie de Québec*).

Competing interests

LF and PG are employed by SCIREQ Inc., a commercial entity with interests in topics related to the content of the present work. YB is holding an operating grant in partnership with SCIREQ Inc. MB, CH, LG, RP and ARR have no conflict of interest.

Additional information

Correspondence and requests for materials should be addressed to Y.B.

Reprints and permissions information is available at www.nature.com/reprints.

Publisher's note Springer Nature remains neutral with regard to jurisdictional claims in published maps and institutional affiliations.

Open Access This article is licensed under a Creative Commons Attribution-NonCommercial-NoDerivatives 4.0 International License, which permits any non-commercial use, sharing, distribution and reproduction in any medium or format, as long as you give appropriate credit to the original author(s) and the source, provide a link to the Creative Commons licence, and indicate if you modified the licensed material. You do not have permission under this licence to share adapted material derived from this article or parts of it. The images or other third party material in this article are included in the article's Creative Commons licence, unless indicated otherwise in a credit line to the material. If material is not included in the article's Creative Commons licence and your intended use is not permitted by statutory regulation or exceeds the permitted use, you will need to obtain permission directly from the copyright holder. To view a copy of this licence, visit <http://creativecommons.org/licenses/by-nc-nd/4.0/>.

© The Author(s) 2024